



HAL
open science

Which Came First: Ventricular Enlargement or Abnormal CSF Circulation?

Pan LIU, Jiachen Xie, Yann Attekeble, Kimi Owashi, Olivier Balédent

► **To cite this version:**

Pan LIU, Jiachen Xie, Yann Attekeble, Kimi Owashi, Olivier Balédent. Which Came First: Ventricular Enlargement or Abnormal CSF Circulation?. 2025 ISMRM & ISMRT Annual Meeting, Proc. Intl. Soc. Mag. Reson. Med., May 2025, Honolulu, France. <10.58530/2025/1063>. <hal-05274008>

HAL Id: hal-05274008

<https://hal.science/hal-05274008v1>

Submitted on 23 Sep 2025

HAL is a multi-disciplinary open access archive for the deposit and dissemination of scientific research documents, whether they are published or not. The documents may come from teaching and research institutions in France or abroad, or from public or private research centers.

L'archive ouverte pluridisciplinaire HAL, est destinée au dépôt et à la diffusion de documents scientifiques de niveau recherche, publiés ou non, émanant des établissements d'enseignement et de recherche français ou étrangers, des laboratoires publics ou privés.



HAL Authorization

1063

Which Came First: Ventricular Enlargement or Abnormal CSF Circulation?

Pan LIU^{1,2}, Jiachen Xie¹, Yann Attekeble³, Kimi Owashi¹, and Olivier Balédent^{1,2}¹CHU Amiens-Picardie, University Hospital, Amiens, France, ²CHIMERE EA.7516, Amiens, France, ³University of Lille, Lille, France

Synopsis

Keywords: Dementia, Neurofluids, Hydrocephalus, CSF Circulation, Brain Morphology, Biomarkers

Motivation: Hydrocephalus involves ventricular enlargement and abnormal CSF circulation. Determining their sequence is crucial for understanding pathogenesis and improving diagnosis.

Goal(s): Validate that area ratio of lateral ventricles to brain (Ratio-Area) and stroke volume ratio of aqueduct to spinal canal (Ratio-SV) are reliable markers, and explore the pathogenesis of communicating hydrocephalus.

Approach: Thirty-six healthy volunteers underwent MRI to extract morphological and fluid dynamics parameters, analysing correlations among aqueduct Resistance, Ratio-Area, and Ratio-SV.

Results: Ratio-Area and Ratio-SV eliminate the influence of heart rate, CSF volume, and brain volume differences. No correlation between Ratio-Area and Ratio-SV, while Resistance showed a strong correlation with Ratio-SV.

Impact: The findings provide insights into the pathogenesis of hydrocephalus, offering potential markers for early diagnosis. Understanding the relationship between aqueduct resistance, Ratio-SV, and Ratio-Area may guide clinical practice and help identify early indicators of CSF dynamic disorders.

Introduction

Communicating normal pressure hydrocephalus (NPH) is characterised by aqueduct dilation (reduced resistance), increased stroke volume at the aqueduct (SV-aq), and enlarged lateral ventricles (Area-vent)¹. Understanding the sequence of these changes is crucial for developing targeted interventions². In NPH patients, these parameters are often already abnormal, making it difficult to determine whether ventricular enlargement causes abnormal CSF circulation or vice versa^{3,4}. Additionally, individual physiological differences, such as heart rate and brain volume, can influence SV-aq and Area-vent, introducing variability. Therefore, using ratios—such as the CSF stroke volume ratio (Ratio-SV) between the aqueduct and second to third cervical (C2-C3), and the area ratio (Ratio-Area) of the lateral ventricles to the brain—may provide more robust physiological markers.

The aim of this study is to quantify aqueduct resistance, Ratio-SV, and Ratio-Area in healthy young adults to demonstrate that these ratios are more suitable metrics for assessing CSF dynamics. Additionally, correlation analysis of these parameters provides insights into the pathogenesis of hydrocephalus.

Methods

Image Acquisition

Thirty-six healthy young volunteers (age 19-35) were examined using a clinical 3T scanner with a 32-channel head coil. Three sequences were acquired: (1) a 3D T1-weighted axial sequence, (2) a balanced fast field echo sequence in the sagittal plane, and (3) a cardiac-gated phase-contrast MRI (PC-MRI) sequence in two planes, both perpendicular to the CSF flow—one at the aqueduct and the other at the spinal canal at C2-C3. Sequence parameters are detailed in Fig.1.

Image Processing

Image processing was conducted using in-house software, Flow 2.0⁵. The steps are illustrated in Fig.2:

1. Segmentation of the lateral ventricles and brain areas was performed on the T1-weighted images to calculate the lateral ventricular area (Area-vent) and the brain area (Area-brain). The Ratio-Area was obtained by dividing Area-vent by Area-brain. The slice with the highest Ratio-Area was selected for further analysis.
2. The aqueduct was segmented using a specialised finite element segmentation platform⁶. Aqueduct resistance was calculated using Poiseuille's law, where Resistance is proportional to the length of the aqueduct and inversely proportional to the fourth power of its diameter.
3. Semi-automatic segmentation was used to extract CSF flow curves in the two planes⁷, and stroke volumes at the aqueduct (SV-aq) and C2-C3 level (SV-cv) were calculated, along with their ratio (Ratio-SV).

Statistical Analysis

Mann-Whitney U tests were used to compare differences between male and female participants for each parameter. Spearman correlation analysis was used to evaluate relationships among the parameters. All statistical analyses were performed using SPSS (version 25), with a significance level of $p < 0.05$.

Results

According to Fig.3, Resistance showed the highest coefficient of variation, especially in males (CV = 91%). Area-brain and SV-cv had lower coefficients of variation (8% and 24%, respectively). Both Ratio-Area and Ratio-SV showed gender differences.

Fig.4 shows that Resistance correlated more strongly with Ratio-Area and Ratio-SV (-0.37 and -0.65, respectively) compared to Area-vent and SV-aq (-0.36 and -0.62, respectively). While SV-aq and SV-cv were influenced by the cardiac period, Ratio-SV was not.

Regardless of gender, there was no correlation between Ratio-Area and Ratio-SV, whereas Resistance was strongly correlated with Ratio-SV (Fig.5).

Additionally, the correlation between Resistance and Ratio-Area showed gender differences, being significant in females ($p=0.006$) but not in males ($p=0.14$).

Discussion

This study demonstrates that morphological and fluid dynamics ratios are robust physiological markers. Ratio-SV reduces the impact of total CSF volume and heart rate, while Ratio-Area mitigates the influence of brain volume. Both Ratio-Area and Ratio-SV showed significant gender differences, highlighting the importance of gender-specific analysis in morphological and fluid dynamics studies. Secondly, unlike results from studies involving NPH patients^{8,9}, no correlation was observed between Ratio-Area and Ratio-SV in healthy volunteers. Incorporating Resistance into the analysis revealed a strong correlation between Resistance and Ratio-SV. These findings suggest that in communicating hydrocephalus, abnormal CSF circulation—initially triggered by reduced aqueduct resistance—may precede and contribute to ventricular enlargement over time.

Conclusion

This study indicates that morphological and fluid dynamics ratios are reliable physiological markers for assessing CSF dynamics. The lack of correlation between Ratio-Area and Ratio-SV, combined with the strong correlation between Resistance and Ratio-SV, suggests that abnormal CSF circulation may play an early role in the progression of communicating hydrocephalus. These findings offer valuable insights into the pathogenesis and diagnosis of hydrocephalus.

Acknowledgements

This research was supported by EquipEX FIGURES (Facing Faces Institute Guiding Research), Hanuman ANR-18-CE45-0014 and Region Haut de France. Thanks to the staff members at the Facing Faces Institute (Amiens, France) for technical assistance. Thanks to David Chechin from Phillips industry for his scientific support.

References

- Wang Z, Zhang Y, Hu F, Ding J, Wang X. Pathogenesis and pathophysiology of idiopathic normal pressure hydrocephalus. *Cns Neurosci Ther.* 2020;26(12):1230-1240. doi:10.1111/cns.13526
- Yamada S, Ishikawa M, Nozaki K. Exploring mechanisms of ventricular enlargement in idiopathic normal pressure hydrocephalus: a role of cerebrospinal fluid dynamics and motile cilia. *Fluids and Barriers of the CNS.* 2021;18(1):20. doi:10.1186/s12987-021-00243-6
- Balédent O, Gondry-Jouet C, Meyer ME, et al. Relationship Between Cerebrospinal Fluid and Blood Dynamics in Healthy Volunteers and Patients with Communicating Hydrocephalus. *Invest Radiol.* 2004;39(1):45. doi:10.1097/01.rli.0000100892.87214.49
- Capel C, Owashi K, Peltier J, Balédent O. Hydrodynamic and Hemodynamic Interactions in Chronic Hydrocephalus. *Biomedicines.* 2023;11(11):2931. doi:10.3390/biomedicines11112931
- Liu P, Fall S, Baledent O. Flow 2.0 - a flexible, scalable, cross-platform post-processing software for real-time phase contrast sequences. In: Vol # 2772. *ISMIR 2022*; 2022. <https://archive.ismrm.org/2022/2772.html>
- Liu P, Owashi K, Metanbou S, Capel C, Balédent O. Using Real Time Phase contrast MRI to investigate CSF oscillations and aqueductal pressure gradients during free breathing. In: *ISMIR 2024*. International Society for Magnetic Resonance in Medicine; 2024. <https://hal.science/hal-04627954>
- Balédent O, Henry-Feugeas MC, C ´cile, Idy-Peretti I. Cerebrospinal Fluid Dynamics and Relation with Blood Flow: A Magnetic Resonance Study with Semiautomated Cerebrospinal Fluid Segmentation. *Investigative Radiology.* 2001;36(7):368-377.
- Chiang WW, Takoudis CG, Lee SH, Weis-McNulty A, Glick R, Alperin N. Relationship Between Ventricular Morphology and Aqueductal Cerebrospinal Fluid Flow in Healthy and Communicating Hydrocephalus. *Invest Radiol.* 2009;44(4):192. doi:10.1097/RLI.0b013e31819a640b
- Vivas-Buitrago T, Lokossou A, Jusué-Torres I, et al. Aqueductal Cerebrospinal Fluid Stroke Volume Flow in a Rodent Model of Chronic Communicating Hydrocephalus: Establishing a Homogeneous Study Population for Cerebrospinal Fluid Dynamics Exploration. *World Neurosurgery.* 2019;128:e1118-e1125. doi:10.1016/j.wneu.2019.05.093

Figures

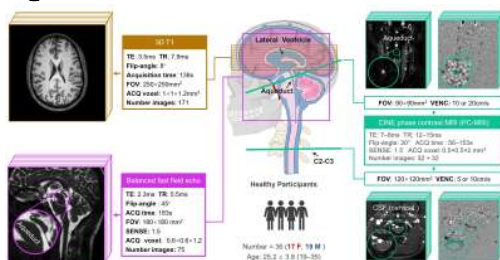


Figure 1: Imaging acquisition and participant information. Imaging locations for the three sequences are shown on the central schematic. Example images and acquisition parameters are color-coded as follows: axial 3D T1 in brown, sagittal balanced fast field echo in purple, and phase contrast (PC-MRI) in cyan, with aqueduct level images on top and C2-C3 level images at the bottom.

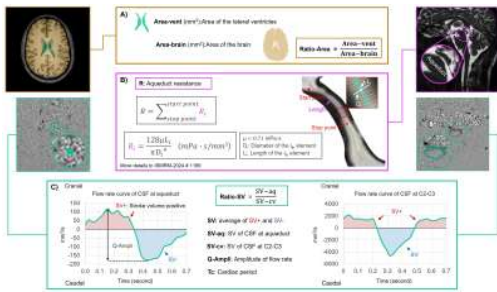


Figure 2: Image processing workflow. A) Lateral ventricles and brain segmentation across multiple slices to extract Area-vent and Area-brain, Ratio-Area calculation, data from the slice with the maximum Ratio-Area was selected. B) Finite element segmentation on the aqueduct to obtain length and diameter, the aqueduct resistance (R) was calculated. C) CSF segmentation at the aqueduct and C2-C3 levels, background correction applied, extraction of the average cardiac cycle flow curve to record stroke volume (SV) and calculate Ratio-SV.

	Age	Cardiac period (milliseconds)	Area-vent (mm²)	Area-brain (mm²)	Ratio-Area (%)	Resistance (mmHg/ml/min)	SV-vent (ml/min)	SV-br (ml/min)	Ratio-SV (%)
Total (n=66)	25.2 ± 3.3	818 ± 125	6.7 ± 2.1	145 ± 11	4.4 ± 1.0	22 ± 24	37 ± 18	602 ± 140	6.2 ± 2.1
Male (n=32)	25.2 ± 3.3	795 ± 98	5.5 ± 0.8	127 ± 15	3.4 ± 0.3	40 ± 25	24 ± 16	480 ± 70	4.1 ± 2.4
CV%	16%	18%	8%	8%	20%	18%	8%	3%	16%
Female (n=34)	26.0 ± 4.2	854 ± 127	6.0 ± 1.9	152 ± 10	4.4 ± 1.4	69 ± 63	51 ± 20	591 ± 153	7.6 ± 3.5
Male (n=32)	22.5 ± 2.8	705 ± 92	4.8 ± 1.3	144 ± 19	5.1 ± 0.2	30 ± 71	27 ± 10	470 ± 70	4.9 ± 0.9
CV%	16%	16%	3%	6%	34%	18%	2%	20%	16%
Female (n=32)	28.2 ± 3.3	174 ± 185	7.4 ± 2.2	139 ± 8	5.5 ± 1.7	75 ± 45	29 ± 12	614 ± 145	4.9 ± 1.9
Male (n=32)	23.0 ± 2.5	706 ± 82	5.4 ± 0.2	135 ± 14	3.7 ± 0.8	50 ± 81	19 ± 10	530 ± 68	2.7 ± 0.8
CV%	14%	14%	3%	8%	31%	65%	42%	23%	16%

	Age	Cardiac period	Area-vent	Area-brain	Ratio-Area	Resistance	SV-vent	SV-br	Ratio-SV
r-value	0.28	0.27	-0.38	0.58	-0.36	-0.22	0.34	-0.27	0.63
p-value	0.34	0.10	0.07	***	0.028*	0.16	0.842*	0.88	0.01**

*** p<0.001, ** p<0.01, * p<0.05

Figure 3: Participant parameters with gender-specific differences. Data are presented as mean ± SD, interquartile range (Q1–Q3), and coefficient of variation (CV). Differences between male and female groups were assessed using the Mann-Whitney test. Violin plots for each parameter by gender are shown at the bottom.

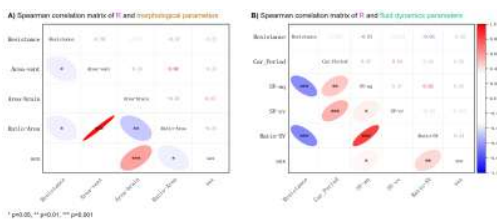


Figure 4: Spearman correlation matrices. The lower triangle shows trend ellipses, and the upper triangle displays effect size (r). p-values are represented at three significance levels. Positive correlations with sex indicate higher values for males than females.

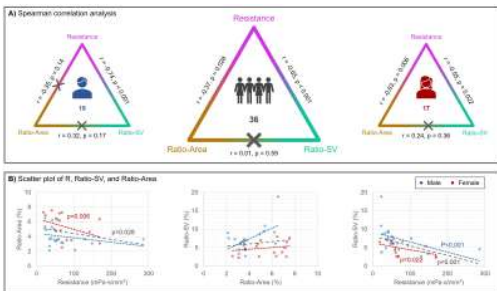


Figure 5: Correlation analysis of Resistance, Ratio-Area, and Ratio-SV. A) Correlation results among the three parameters, with gender differentiation. B) Scatter plots of pairwise relationships between the three parameters, color-coded by gender. The grey trend line represents the overall trend, and significant correlations are marked with p-values. Ratio-Area denotes the proportion of ventricular area, and Ratio-SV denotes the proportion of stroke volume in the aqueduct.